

DISPERSION PROPERTIES OF $\text{GaSe}_{1-x}\text{S}_x$ IN THE TERAHERTZ RANGE

Lai-Ming Zhang,^a Jin Guo,^a Dian-Jun Li,^a Ji-Jiang Xie,^a
Yu. M. Andreev,^b V. A. Gorobets,^c V. V. Zuev,^b
K. A. Kokh,^d G. V. Lanskii,^b V. O. Petukhov,^{c*}
V. A. Svetlichnyi,^e and A. V. Shaiduko^b

UDC 535.323-14;621.378.32

We grew nonlinear crystals of the solid solutions $\text{GaSe}_{1-x}\text{S}_x$ ($x \leq 0.4$) by the vertical Bridgman method. The increase in hardness from 8 kg/mm^2 for $x = 0$ to $\sim 20 \text{ kg/mm}^2$ for $x = 0.4$ as a result of the presence of sulfur in the GaSe crystals allowed us to use a special technology to make working samples with position of the optic axis in the plane of the entrance surfaces, and for the first time to make direct measurements of the dispersion properties $n_e(\lambda)$ for the extraordinary wave and $n_o(\lambda)$ for the ordinary wave in the terahertz range of the spectrum by pulsed terahertz spectroscopy. We show that it is possible to realize an unconventional ee–e type of interaction in generation of terahertz radiation.

Keywords: nonlinear crystal optics, parametric frequency conversion, GaSe, crystal of solid solutions, terahertz radiation.

Introduction. The unique set of physical properties in nonlinear GaSe crystals, responsible for the efficiency of parametric frequency conversion processes for converting radiation in the near IR and mid-IR ranges to the terahertz range of the spectrum [1, 2], has attracted steady attention from many researchers and developers. Unfortunately, the extremely poor mechanical properties (almost zero hardness on the Mohs scale and easy cleavage) limit use of these layered crystals of symmetry point group $\bar{6}2m$ to intralaboratory applications.

Recently, with the aim of expanding nonlinear optics applications, the mechanical properties of GaSe crystals have been significantly improved as a result of doping with Group III and Group IV elements of Mendeleev's Periodic Table (Al [3], S [4], In [5–7], Te [8, 9], Er [10]) and growing the corresponding crystals of the solid solutions, and also by growing crystals from GaSe:AgGaSe_2 [6] and GaSe:AgGaS_2 [11] melts. In contrast to GaSe crystals, AgGaSe_2 and AgGaS_2 crystals have symmetry point group $\bar{4}2m$. It has been established that besides the mechanical properties, other key physical properties of GaSe crystals can be controllably modified by selection of the sulfur content. Introducing large concentrations of sulfur, indium, and tellurium (leading to a change in the lattice parameters) have the best possibilities in this regard; in other words, growing nonlinear crystals of solid solutions according to the chemical formulas $\text{GaSe:GaS} \rightarrow \text{GaSe}_{1-x}\text{S}_x$ [4], [12–19], $\text{GaSe:InSe} \rightarrow \text{Ga}_{1-x}\text{In}_x\text{Se}$ [5, 7], and $\text{GaSe:GaTe} \rightarrow \text{GaSe}_{1-x}\text{Te}_x$ [8, 9]. Introducing small sulfur ions eliminates cleavage defects in the GaSe crystals and reduces linear optical losses in the region of maximum transparency (optimal doping level, 2–3 wt.%), and also increases the thermal conductivity several-fold orthogonal to the growth layers, as a result of substitution of selenium ions, filling vacancies, and intercalation in the interlayer space. As a result of these changes, the radiation resistance relative to nanosecond pump pulses increases by 20%–30%. The increase in the mixing ratio to $x \leq 0.4$ shifts the short-wavelength edge of the transmission spec-

*To whom correspondence should be addressed.

^aChangchun Institute of Optics, Fine Mechanics and Physics, Chinese Academy of Sciences; e-mail: lightcoming@ciomp.ac.cn; ^bInstitute for Monitoring Climatic and Ecological Systems, Siberian Branch, Russian Academy of Sciences, 10/3 Akademicheskii Ave., Tomsk 634021; e-mail: yuandreev@imces.ru; ^cB. I. Stepanov Institute of Physics, National Academy of Sciences of Belarus, 68 Nezavisimosti Ave., Minsk 220072; e-mail: v.petukhov@ifanbel.bas-net.by; ^dInstitute of Mineralogy and Geology, Siberian Branch, Russian Academy of Sciences, Novosibirsk; e-mail: k.a.kokh@gmail.com; ^eTomsk State University, Russia; e-mail: v_svetlichnyi@rambler.ru. Translated from Zhurnal Prikladnoi Spektroskopii, Vol. 77, No. 6, pp. 915–921, November–December, 2010. Original article submitted August 10, 2010.

trum of the nonlinear crystals of solid solutions $\text{GaSe}_{1-x}\text{S}_x$ from 0.62 m to 0.54 μm , while simultaneously shifting the phase matching curves for parametric frequency conversion processes. The shift of the edge of the transmission spectrum toward shorter wavelengths significantly reduces the level of linear and also nonlinear optical losses at short pump wavelengths: emission of dye lasers ($\lambda = 0.60\text{--}0.75 \mu\text{m}$), Nd:YAG (1.06 μm), femtosecond titanium:sapphire (0.7–1.1 μm) and chromium:forsterite (1.25–1.32 μm) lasers. In turn, a decrease in the phase matching angles leads to a corresponding increase in the effective nonlinear susceptibility of negative GaSe crystals [4]. With respect to all the modified properties of the nonlinear crystals of solid solutions $\text{GaSe}_{1-x}\text{S}_x$, an efficiency of second harmonic generation for an erbium laser has been demonstrated that is 2.4 times higher than that of pure GaSe crystals [4], while for crystals grown from a GaSe:AgGaSe_2 melt, the frequency doubling efficiency for a CO_2 laser is four times greater than for ZnGeP_2 crystals.

Efficient use of nonlinear crystals of solid solutions (NCSS) $\text{GaSe}_{1-x}\text{S}_x$ within parametric frequency converters, including for conversion of the frequency to the THz range of the spectrum, is not possible without knowing the dispersion properties, which are difficult to determine for a number of reasons. The expression for determining the dispersion properties of crystals of solid solutions with respect to the known dispersion properties of the original crystals [20], written as applied to the case under consideration in the form

$$n_{o,e}^2(\text{NCSS GaSe}_{1-x}\text{S}_x) = (1 - x) n_{o,e}^2(\text{GaSe}) + x n_{o,e}^2(\text{GaS}),$$

cannot be used in practice due to differences between the polytype structures of the bulk crystals of ϵ -GaSe and ϵ - $\text{GaSe}_{1-x}\text{S}_x$ ($x \leq 0.4$) [4], on the one hand, and β -GaS [21] on the other hand, grown by the only possible Bridgman method. Therefore the dispersion properties have been determined only for the ϵ polytype of GaSe [22] and the β polytype of GaS [23]. From known data, it follows that GaS crystals, existing in pure form as the β polytype, match the structure of ϵ -GaSe and are transformed to the ϵ polytype which is possible for them, incorporated into the solid solution ϵ - $\text{GaSe}_{1-x}\text{S}_x$, $x \leq 0.4$. Application of the original nonlinear optics method proposed in [16] for determining the dispersion properties of nonlinear crystals of solid solutions ϵ - $\text{GaSe}_{1-x}\text{S}_x$, $x \leq 0.4$, using corrected data on the dispersion properties of β -GaS crystals, was justified. The region of their applicability was established, 0.63–20 μm [23] and (only for the eo-e interaction) the THz range [16].

Note that widely used data on the dispersion properties of ϵ -GaSe crystals in the IR range [10], obtained by indirect methods, are insufficiently correct and are still being refined. In one recent paper [24], direct measurements of the refractive indices n_e and n_o of the GaSe crystals are reported, using a prism made after casting in a polymerizing compound. The values of n_e and n_o were determined in the subranges 0.7–1.4 μm and 2.4–5.0 μm using the minimum deviation method. Thus the lack of data on direct measurements of the dispersion properties of the original ϵ -GaSe crystals and the lack of bulk ϵ -GaS crystals had not made it possible to date to obtain adequate information about the dispersion properties of nonlinear crystals of solid solutions ϵ - $\text{GaSe}_{1-x}\text{S}_x$ in the THz range using expression (1).

Considering the fact that nonlinear crystals of solid solutions $\text{GaSe}_{1-x}\text{S}_x$ have demonstrated good operating characteristics within application-oriented devices in the mid-IR range [15–19] and are suitable for machining to a greater extent than GaSe and GaS crystals, the aim of this work was to make working samples and to directly determine the dispersion properties $n_e(\lambda)$ and $n_o(\lambda)$ of the nonlinear crystals of solid solutions ϵ - $\text{GaSe}_{1-x}\text{S}_x$, $x \leq 0.4$ in the THz range of the spectrum.

Fabrication and Characteristics of the Crystals. The basic starting elements for the GaSe crystals grown by the vertical Bridgman method were special-purity Ga (99.9999) and Se (99.9999). Sulfur (99.9) was introduced within the range 0.1–10 wt.% ($x \leq 0.412$) by direct addition to the selenium mix. The temperature gradient of the solidification front was 10 degrees/cm with a pull rate of 6 mm/day. The crystals were not subjected to post-growth treatment.

Characterization of the grown crystals by the procedure in [4] showed that they have an asymmetric structure of the ϵ polytype and are suitable for nonlinear optics applications. The level of the optical loss coefficient within the maximum transparency window in the mid-IR range, $\alpha \leq 0.1\text{--}0.2 \text{ cm}^{-1}$, corresponds to the modern state of the art in the technology for growing pure [2] and sulfur-doped [4] GaSe crystals. The microhardness of the (001) surface of the grown crystals was measured using a PMT-3 microhardness tester. We established that as a result of introducing sulfur, the hardness increased from 8 kg/mm^2 for $x = 0$ up to $\sim 20 \text{ kg/mm}^2$ for $x = 0.4$.

The optic axis in layered pure and doped GaSe crystals is directed orthogonal to the growth layers. The increase in hardness significantly simplifies machining, but it still leads to chipping of the crystals. In order to eliminate

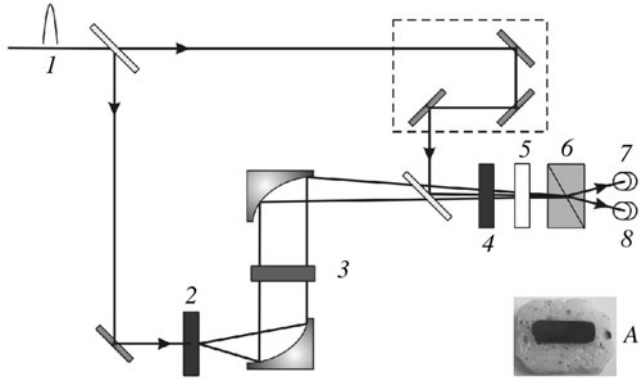


Fig. 1. Optical block diagram of the terahertz range spectrometer: 1) pulse from a femtosecond laser (dashed lines show the optical delay line), 2) dipole antenna based on a $10 \times 10 \times 1$ mm InP crystal, 3) test sample of $\text{GaSe}_{1-x}\text{S}_x$, 4) electro-optic detector mad from ZnTe (110) of dimensions $10 \times 10 \times 2$ mm, 5) quarter-wave plate, 6) Wollaston prism, 7, 8) Si diodes; A is a polished sample of the $\text{GaSe}_{1-x}\text{S}_x$ crystal.

such chipping, before fabrication of working elements from GaSe and $\text{GaSe}_{1-x}\text{S}_x$ with an optic axis in the plane of the entrance surfaces, the single-crystalline ingots were cast in an easily removable (as needed) silicone potting compound, and then coated with a layer of high-strength epoxy resin. In another variant, we used a specially selected polymerizing compound with a low (fraction of a percent) shrinkage factor on curing. The best results came from slicing the ingot with a diamond strip of thickness $10 \mu\text{m}$ under its own weight (Fig. 1, A) and a wire impregnated with fine Al_2O_3 dust, which was also used to polish the surfaces of the slice. In contrast to diamond dust, Al_2O_3 dust residues are easily removed by brief chemical etching. Additional final grinding of the working surfaces of the crystals heated up to 300°C was done in an evacuated container with residual pressure $3 \cdot 10^{-6}$ torr, with the help of laser ablation using a KrF excimer laser (pulse repetition frequency 3 Hz, pulse energy 0.5 J with beam diameter 4 cm at the 10% level). We used a Solver HV atomic force microscope to establish that the height of asperities on the polished surfaces is no more than 15–20 nm. This is approximately an order of magnitude better than for surfaces of crystals prepared by the cleavage method.

The Experiment. In order to determine the dispersion properties of the studied crystals, we assembled a conventional apparatus for pulsed time-domain THz transmission spectroscopy (Fig. 1).

The THz spectrometer essentially operates as follows. As the main radiation source, it uses a femtosecond titanium:sapphire laser ($\lambda_{\text{rad}} = 800$ nm, pulse duration 120 fs, pulse repetition frequency 1 kHz, single pulse energy 400 μJ), the linearly polarized output beam from which is split into two parts. The first beam excites the dipole source of THz radiation based on an InP crystal, and an optical system of off-axis paraboloid mirrors guides the isolated THz radiation to the test crystal and then to the electro-optic detector made from ZnTe. The InP crystal is simultaneously a band-rejection filter for residual radiation of the first beam. The second beam, after passing through the computer-controlled optical delay line, is also fed to the entrance of the electro-optic detector. After making it coincide, within the volume of the electro-optic detector, with the THz radiation by controlling the delay time and subsequent interaction, the second beam changes the direction of polarization in proportion to the amplitude of the THz radiation as a result of the electro-optic effect. This occurs because the wavelength of the THz radiation significantly exceeds the wavelength of the emission from the titanium:sapphire laser, and is perceived by it as a static electric field. At the exit from the quarter-wave plate mounted next in line, this radiation beam at $\lambda = 800$ nm becomes elliptically polarized. Its two orthogonal components are separated in the Wollaston prism and fed to the input of the differential Si diode system. The electrical signal from the output of the differential system, also proportional to the amplitude of the THz radiation, is fed to the input of the lock-in amplifier and then to the display system.

During the measurements, by controlling the delay time of the optical line we determined the temporal shape of the THz pulses and the time Δt it takes the main peak of the THz pulse to pass through the measurement circuit

in the absence of the test sample of the crystal (reference signal) and when the sample is mounted in the measurement circuit. From the measured time it takes the main radiation peak to pass through it, using the expression

$$n_g = 1 + (c\Delta t/d), \quad (1)$$

where c is the speed of light, d is the thickness of the crystal, we calculated the group refractive index n_g of the test crystals.

In principle, the pulsed time-domain THz spectroscopy method allows us to obtain, in a single experiment, the spectral dependence of the complex refractive index

$$\tilde{n} = n + ik, \quad (2)$$

where n is the real refractive index; k is the attenuation coefficient. Using the inverse Fourier transform method to find the spectral distribution of the amplitudes $E_0(\omega)$ and $E_T(\omega)$ for the reference THz pulse and the THz pulse passing through the object, we can determine the spectral dependence of the transmission coefficient T and the phase difference Δ between the spectral components of the signal and reference pulses. Then

$$\frac{E_T(\omega)}{E_0(\omega)} = T \frac{e^{i\tilde{n}\omega d/c}}{e^{i\omega d/c}} = \frac{4\tilde{n}}{(\tilde{n}+1)^2} e^{i(\tilde{n}-1)\omega d/c}, \quad (3)$$

$$E_T(\omega)/E_0(\omega) = A e^{-i\Delta}, \quad (4)$$

where A is the ratio of the amplitudes of the detected THz pulses. In the case of low absorption ($n \gg k$), from expressions (3) and (4) the dispersion properties in the THz range are determined as

$$n(v) \approx 1 + (c\Delta)/(\omega d) = 1 + (c\Delta/2\pi v d). \quad (5)$$

Figure 2 shows an example of the dispersion dependences for pure and sulfur-doped GaSe crystals in the THz range, calculated from expression (5) taking into account the measurement results obtained. Here we also show the results of model calculations using the familiar dispersion equations in [22, 25]. The spectral dependences of the dielectric properties of GaSe and $\text{GaSe}_{1-x}\text{S}_x$ crystals are obtained in the frequency range 0.2–2.0 THz.

Discussion of Results. From Fig. 2 we see that the results of measurement of the dispersion $n_o(\lambda)$ agree well both with numerical estimates made based on the dispersion equations in [26] and with its average value of 3.26, calculated from formula (1). The position of the sliding phonon mode in the 0.59 THz region corresponds well to known data in [10]. There is a marked difference between the measured values of $n_o(\lambda)$ and the results of estimates from the dispersion expressions in [23], with sufficiently good agreement with the calculated data in [10]. We should point out that in [10], the results are obtained for erbium-doped GaSe crystals with signs of degradation of the crystal lattice: there are elements of transformation of the transmission spectrum and broadening of the rocking curve. Most likely it is specifically these data that should differ more from the results obtained. However, in practice, both expressions give sufficiently close values for determination of the phase matching angles for parametric frequency conversion processes in the THz range of the spectrum. This can be explained by a decrease in the effect of the vector \mathbf{k}_1 (with maximum wavelength) in the vector sum $\mathbf{k}_1 + \mathbf{k}_2 = \mathbf{k}_3$, defining one of the phase matching conditions: the law of conservation of momentum (here \mathbf{k}_2 and \mathbf{k}_3 are the wave vectors for waves with an intermediate wavelength and a wavelength that is as short as possible). Therefore a marked difference between the dispersion dependences in the THz range only slightly affects the results of calculation of the phase matching conditions, and gives considerable uncertainty in the inverse process: determination of the dispersion properties from the measured phase matching angles.

On the $n_e(\lambda)$ dependence, the absorption peak for the sliding phonon mode for GaSe crystals was not observed as in both $n_o(\lambda)$ and $n_e(\lambda)$ dependences for the nonlinear crystal of solid solutions $\text{GaSe}_{1-x}\text{S}_x$. The latter circumstance indicates strengthening of interlayer bonds, which increase interlayer interaction and suppress the sliding phonon mode, promoting an increase in the efficiency of generation of THz radiation of e polarization. From Fig. 2, we also see that with an increase in the sulfur content, the birefringence of the nonlinear crystal of solid solutions $\text{GaSe}_{1-x}\text{S}_x$ is practically unchanged: ~0.77.

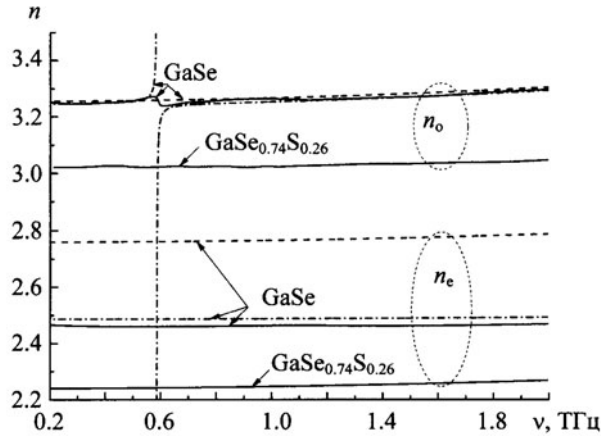


Fig. 2. Dispersion dependences for the ordinary n_o and extraordinary n_e waves in GaSe and $\text{GaSe}_{0.74}\text{S}_{0.26}$ crystals; solid lines indicate the experimental data, the dashed line and the broken line indicate data from model calculations using the familiar dispersion equations from [22, 25].

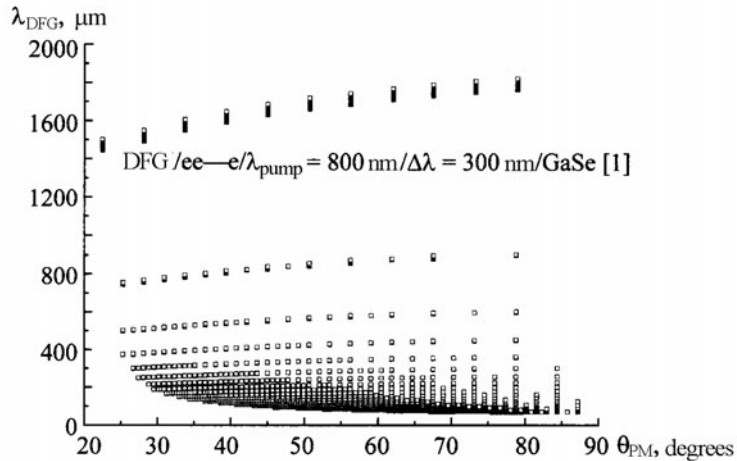


Fig. 3. Phase matching conditions for difference frequency generation in different spectral sections of a titanium:sapphire laser in GaSe crystals.

Model studies showed that the unusual dispersion properties of all the studied crystals allow us to realize an unconventional ee–e type of three-wave interaction for short-wavelength pump sources (Fig. 3). In calculations of the dependences of the radiation wavelength on the difference frequency λ_{DFG} on the phase matching angle θ_{PM} (Fig. 3), it is assumed that the wavelength of the titanium:sapphire laser is 800 nm, the spectral bandwidth of the radiation is 30 nm, the spectrum of the radiation is separated into 200 sections taken as the spectral width of independent radiation sources for which difference frequencies are generated in the GaSe crystals. We analyzed all possible variants for difference frequency generation; the total number of them is equal to the number of combinations of 200 taken 2 at a time. From Fig. 3, we see that in this case, the ee–e type of frequency mixing makes it possible to span broad spectral sections of 80–900 and 1410–1800 μm . We have also established that introducing sulfur, as for the heavier elements (indium and tellurium), enriches the phonon absorption spectrum but, in contrast to the latter elements, shifts them toward shorter wavelengths. In all cases, the absorption coefficient for the extraordinary wave considerably exceeds (by a factor of 10 or more) the absorption coefficient for the ordinary wave. The difference is increased as the wavelength decreases.

Conclusion. Securing samples of nonlinear crystals of solid solutions $\text{GaSe}_{1-x}\text{S}_x$ in a holder made of polymerizing compounds and followed by machining, according to our technology, made it possible to make samples of crystals of solid solutions with the optic axis in the plane of the entrance surfaces. Using pulsed terahertz spectroscopy (for the first time, according to our data), we have studied the dispersion properties of nonlinear optical crystals of GaSe and $\text{GaSe}_{1-x}\text{S}_x$ for ordinary and extraordinary waves in the frequency range 0.2–2.0 THz. The good correspondence between the numerical modeling results and the use of familiar expressions for the dispersion properties of pure GaSe crystals and the experimental data confirm the validity of the results obtained even for $\text{GaSe}_{1-x}\text{S}_x$ crystals whose polished entrance surfaces are characterized by higher optical quality owing to greater hardness. The data obtained can be used in developing dispersion equations for $\text{GaSe}_{1-x}\text{S}_x$ crystals. For the first time, we have established that in pure GaSe crystals and nonlinear crystals of solid solutions $\text{GaSe}_{1-x}\text{S}_x$, it is possible to realize an unconventional ee–e type of interaction.

We would like to thank the following for partial financial support: the Presidium of the National Academy of Sciences of Belarus and the Siberian Branch of the Russian Academy of Sciences, within the joint basic research project of the National Academy of Sciences of Belarus and the Siberian Branch of the Russian Academy of Sciences No. 10 of 2010, the Russian Foundation for Basic Research within project No. 10-02-01452-a, the Federal Special Program on "Scientific and scientific educational innovation groups in Russia" within government contract No. 02.740.11.0444, NSh-4297.2010.2, Jilin Provincial Science and Technology Department, Grant 2008070.

REFERENCES

1. V. G. Dmitriev, G. G. Gurzadyan, and D. N. Nikogosyan, *Handbook for Nonlinear Optical Crystals*, Springer, Berlin (1999).
2. Y.-S. Lee, *Principles of Terahertz Science and Technology*, Springer, New York (2008).
3. A. A. Tikhomirov, Yu. M. Andreev, G. V. Lanskii, O. V. Voevodina, and S. Yu. Sarkisov, *Proc. SPIE*, **6258**, 64–72 (2006).
4. H.-Z. Zhang, Z.-H. Kang, Yu. Jiang, J.-Yu. Gao, F.-G. Wu, Z.-S. Feng, Yu. M. Andreev, G. V. Lanskii, A. N. Morozov, E. I. Sachkova, and S. Yu. Sarkisov, *Opt. Express*, **16**, No. 13, 9951–9957 (2008).
5. D. R. Suhre, N. B. Singh, V. Balakrishna, N. C. Fernelius, and F. K. Hopkins, *Opt. Lett.*, **22**, No. 11, 775–777 (1997)
6. N. B. Singh, D. R. Suhre, W. Rosch, R. Meyer, M. Marable, N. C. Fernelius, F. K. Hopkins, D. E. Zelmon, and R. Narayanan, *J. Cryst. Growth*, **198**, 588–592 (1999).
7. Z.-S. Feng, Z.-H. Kang, F.-G. Wu, J.-Yu. Gao, Yu. Jiang, H.-Z. Zhang, Yu. M. Andreev, G. V. Lanskii, V. V. Atuchin, and T. A. Gavrilova, *Opt. Express*, **16**, No. 13, 9978–9985 (2008).
8. K. C. Mandal, S. H. Kang, M. Choi, J. Chen, Xi-Ch. Zhang, J. M. Schleicher, C. A. Schmuttenmaer, and N. C. Fernelius, *IEEE J. Sel. Top. Quantum Electron.*, **14**, No. 2, 284–288 (2008).
9. Yu. M. Andreev, G. V. Lanskii, S. N. Orlov, and Yu. N. Polivanov, in: *Abstracts, Seventeenth International Conference on Advanced Laser Technologies*, 26 September–1 October 2009, Kossaeli, Turkey (2009), p. 55.
10. Y.-K. Hsu, C.-W. Chen, J. Y. Huang, C.-L. Pan, J.-Y. Zhang, and C.-S. Chang, *Opt. Express*, **14**, No. 12, 5484–5491 (2006).
11. O. Yu. Khyzhun, Yu. M. Andreev, V. V. Atuchin, N. F. Beizel, and L. D. Pokrovsky, in: *Abstracts, Eleventh International Conference on Crystal Growth of Intermetallic Compounds*, Lvov, Ukraine, 30 May–2 June 2010, ICDD, Lvov (2010), p. 103.
12. Yu. M. Andreev, V. V. Atuchin, G. V. Lanskii, A. N. Morozov, L. D. Pokrovsky, S. Yu. Sarkisov, and O. V. Voevodina, *Mater. Sci. Eng. B*, **128**, 205–210 (2006).
13. S. Das, C. Ghosh, O. Voevodina, Yu. M. Andreev, and S. Yu. Sarkisov, *Appl. Phys. B*, **81**, No. 8, 43–46 (2006).
14. T.-J. Wang, J.-Y. Gao, Yu. M. Andreev, V. V. Atuchin, T. N. Kopylova, G. V. Lanskii, T.D. Malinovskaya, L. D. Pokrovskii, and S. Yu. Sarkisov, *Izv. Vuzov. Fizika*, No. 6, 35–40 (2007).
15. Y. Qu, Z.-H. Kang, T.-J. Wang, Y. Jiang, J.-Y. Gao, and Yu. M. Andreev, *Laser Phys. Lett.*, **4**, No. 3, 238–241 (2007).

16. Y. Qu, Z.-H. Kang, T.-J. Wang, Yu. M. Andreev, G. V. Lanskii, A. N. Morozov, and S. Yu. Sarkisov, *Opt. Atm. Okeana*, **21**, No. 2, 170–175 (2008).
17. S.-A. Ku, C.-W. Luo, H.-L. Lio, K.-H. Wu, J.-Y. Juang, A. I. Potekaev, O. P. Tolbanov, S. Yu. Sarkisov, Yu. M. Andreev, and G. V. Lanskii, *Izv. Vuzov. Fizika*, **51**, No. 10, 80–85 (2008).
18. G. V. Maier, T. N. Kopylova, Yu. M. Andreev, V. A. Svetlichnyi, and E. N. Tel'minov, *Izv. Vuzov. Fizika*, No. 6, 83–88 (2009).
19. Yu. M. Andreev, M. N. Baldin, V. M. Gruznov, V. A. Kapitanov, A. L. Makas', Yu. N. Ponomarev, E. L. Schastlivtsev, O. V. Tailakov, A. A. Tikhomirov, and M. L. Troshkov, *Opt. Atm. i Okeana*, **22**, No. 1, 74–81 (2009).
20. M. S. Webb, D. Eimerl, and S. P. Velsko, *J. Opt. Soc. Am. B*, **9**, No. 7, 1118–1127 (1992).
21. N. C. Fernelius, *Prog. Cryst. Growth and Charact.*, **28**, 275–353 (1994).
22. K. L. Vodopyanov and L. A. Kulevskii, *Opt. Commun.*, **118**, 375–378 (1995).
23. K. R. Allakhverdiev, R. I. Guliev, É. Yu. Salaev, and V. V. Smirnov, *Kvant. Elektron.*, **9**, No. 7, 1483–1485 (1982).
24. K. R. Allakhverdiev, T. Baukara, A. Kulibekov Gulubayov, A. A. Kaya, J. Goldstein, N. Fernelius, S. Hanna, and Z. Salaeva, *J. Appl. Phys.*, **98**, 093515-1-6 (2005).
25. C.-W. Chen, T.-T. Tang, S.-H. Lin, J. Y. Huang, C.-S. Chang, P.-K. Chung, S.-T. Yen, and C.-L. Pan, *J. Opt. Soc. Am. B*, **26**, No. 9, A58–A65 (2009).
26. W. Shi and Y. J. Ding, *Appl. Phys. Lett.*, **84**, No. 10, 1635–1637 (2004).